ARCHIVES of FOUNDRY ENGINEERING

Published quarterly as the organ of the Foundry Commission of the Polish Academy of Sciences

ISSN (1897-3310)
Volume 13
Special Issue
3/2013

161 – 166

31/3

Numerical Analysis of Solid Particles Flow in Liquid Metal

M. Szucki [a]*, T. Goraj [b], J. Lelito [c], J.S. Suchy [d]
[a-d] AGH University of Science and Technology. Faculty of Foundry Engineering.
23 Reymonta Street, 30-059 Krakow, Poland
*Corresponding author. E-mail address: mszucki@agh.edu.pl

Received 20.10.2013; accepted in revised form 12.12.2013

Abstract

The aim of the study was to determine the influence of the solid particles density and size on their distribution in the solidified cast. As part of the work, a series of numerical simulations of filling and solidification process were made with the use of FLOW-3D software. The analysis was performed on pure aluminum and six chosen types of particles with different size and density. Obtained results may help to understand the behavior of solid particles in liquid metals.

Keywords: numerical analysis, solid particles, particle flow, Metal Matrix Composite, FLOW-3D.

o

1. Introduction

One of the most important factors which determine quality of the cast is the mould filling. During this process liquid alloy often carries some solid particles of various type, shape or size, such as: non-metallic inclusions, particles of the reinforcing phase (in composites) and granules of moulding materials. Those particles can influence casting properties in both a positive and negative way. Reinforcing particles in Metal Matrix Composite (MMC) strengthen alloy structure, therefore their homogeneous distribution in the cast is required [1-4]. On the other hand small solid object like sand grains are treat as unwanted contaminants. In this case, such particles should be prevent from getting into the mould cavity. Thus, its highly important to understand behavior of solid particles in liquid metals.

2. Numerical analysis

Tracking of solid particles in liquid metals poses many problems in both laboratory and industrial. Observation is complicated by the high temperature and non-transparent mould materials. Usually it is only possible to verify final distribution of particles in a solid cast. For this reason, in this study computer simulations were used [5-6]. The Figure 1 shows a model system consisting of runner and three casts in form of plates.

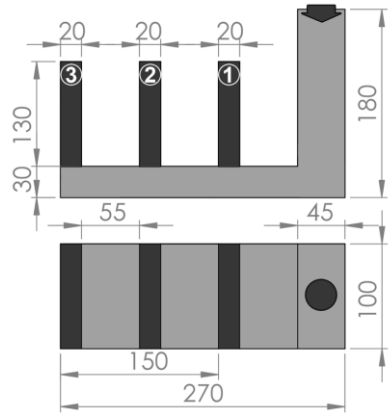

Fig. 1. Schematic introduction of model system;
light gray - gating system, dark gray - casts, arrow - inlet area

Table 1.
Particles types

density \ diameter	10 [μm]	100 [μm]
1350 [kg/m^3]	**Type A10**	**Type A100**
2700 [kg/m^3]	**Type B10**	**Type B100**
5400 [kg/m^3]	**Type C10**	**Type C100**

Simulations were performed for pure aluminum and six types of solid particles differing in size and density according to Table 1. At the same time variation of density and particle diameter for each of those types were neglected.

Table 2.
Parameters numerical simulation

Liquid density (pure aluminum)	2700 [kg/m^3]
Liquid dynamic viscosity (pure aluminum)	0.0013 [Pa*s]
Liquid thermal conductivity (pure aluminum)	96.4 [W/(m*K)]
Liquid specific heat (pure aluminum)	1086 [J/(kg*K)]
Melting point (pure aluminum)	660 [°C]
Filling temperature	680 [°C]
Filling time	5.5 [s]
Latent heat (pure aluminum)	397,5 [kJ/kg]
Initial mould temperature	20 [°C]
Mould material	Green sand
Gravity	9.81 [m/s^2]

Authors used well known commercial simulation environment FLOW-3D to ensure proper fluid-particle interactions [7]. Studies were performed based on gravity, sand casting. The analysis covers the particle flows during filling and solidification process.

The parameters used in numerical simulation are summarized in Table 2. The computations were carried out until all of the plates were solid (solid fraction in the plates was equal to 1).

3. Results and discussion

Two dimensional particle distribution on the plane passing through the center of model system as well as particle concentration in three-dimensional space were analyzed. On the figures included in this work, particles were rescaled (which did not affect the simulation) in order to improve their visibility.

3.1. Particles type A

The Figure 2a and 2b shows comparison of the particles type A100 distribution: after 5.5 [s] from the start of the simulation (right after the filling was completed) and after 150 [s] (when plates were completely solidified).

It is clearly visible that particles with smaller density than liquid metal are floating to the top of the system from early beginning of mould filling.

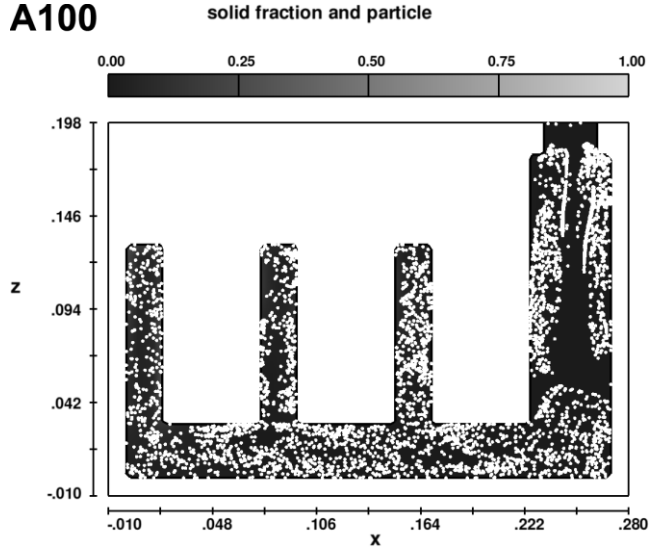

Fig. 2a. Two dimensional distribution of particles type A100 (white points) after 5.5 [s]

This motion continues when the mould is completely filled and the process of cooling and solidification starts. At the same time the final distribution of particles in the system strongly depends on the alloy temperature and the cooling rate [8]. After filling, temperature in the part of cast located farther from inlet is lower, which means that crystallization process may finish earlier in such area. Thus, particles have less time to flow up, which explains more

uniform distribution in plates 3 and 2 than in plate 1 (where temperature is higher and the cooling rate lower due to sprue neighborhood).

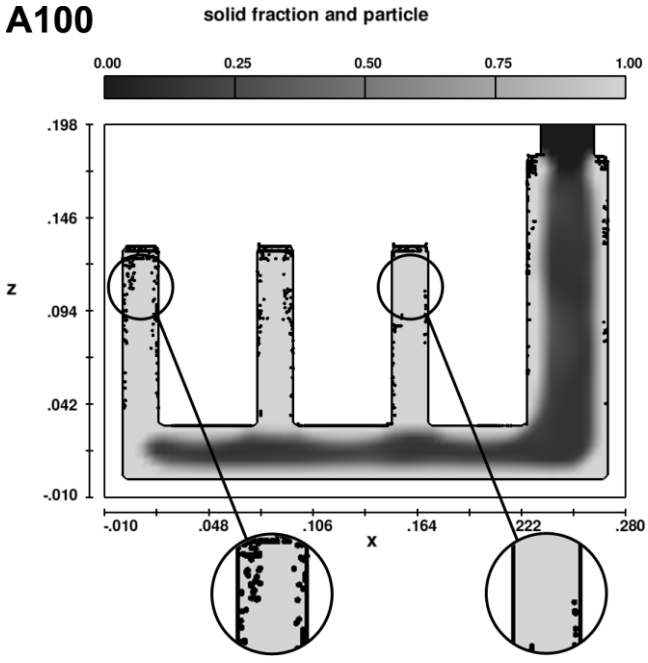

Fig. 2b. Two dimensional distribution of particles type A100 (black points) after 150 [s]; Visible magnification of selected areas of the plates

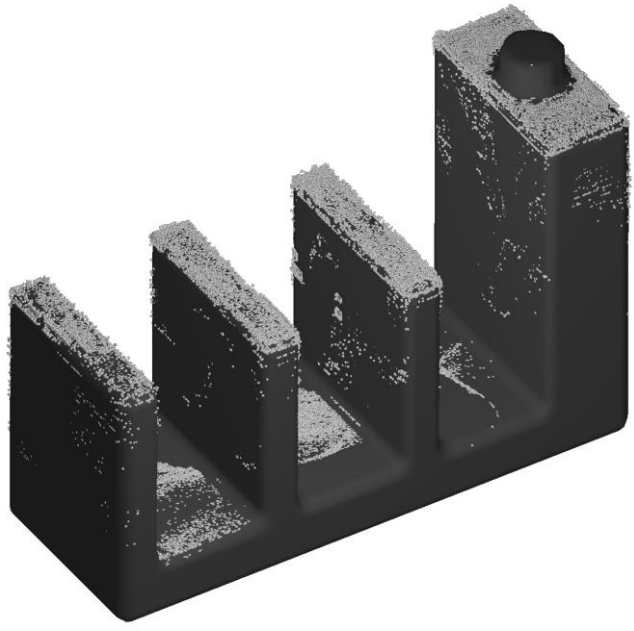

Fig. 3. Three dimensional distribution of particle A100 (white point) on the top of model system after 150 [s]

Particle concentration variations for the upper part of each plate are clearly visible on three dimensional visualization of simulation results shown in Figure 3.

In order to confirm presented explanation of this phenomenon, analysis of fraction solid changes in the geometric center of each plate was made. As shown in Fig. 4 most significant differences in solidification time occurs between the plate No. 3 and 1. This translates directly into the particles distribution differences in these areas.

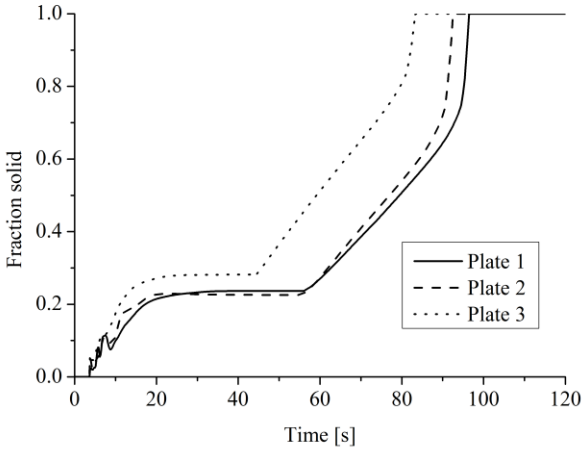

Fig. 4. Comparison of fraction solid changes for each plate as a function of time

For the particle type A10 (Fig. 5a) after completion of the filling process, the distribution is similar to the A100 at the same time stage.

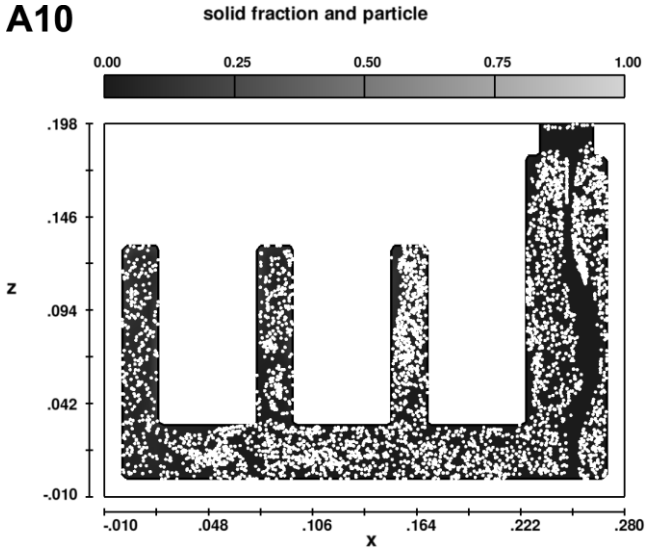

Fig. 5a. Two dimensional distribution of particles type A10 (white points) after 5.5 [s]

However, since the particles diameter is smaller (10 μm) floating speed is also smaller. Thus, after solidification uniform distribution in the casting could be observed (Fig.5b).

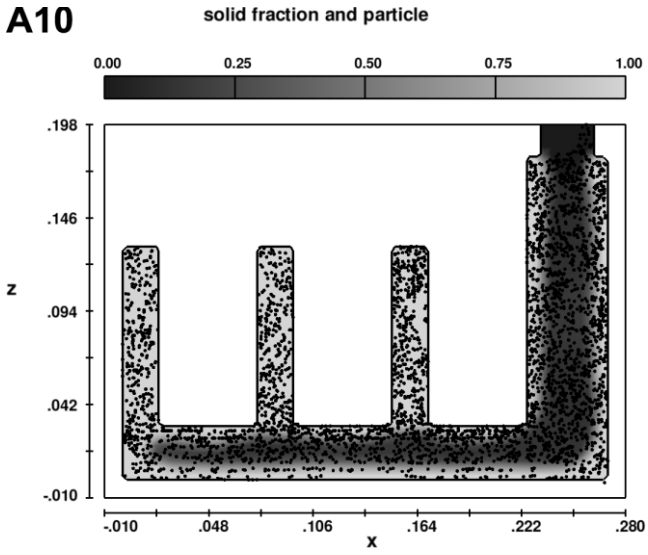

Fig. 5b. Two dimensional distribution of particles type A10 (black points) after 150 [s]

As the liquid and particles have the same density, the movement of this second phase after filling is directly related with the convection flows in liquid metal.

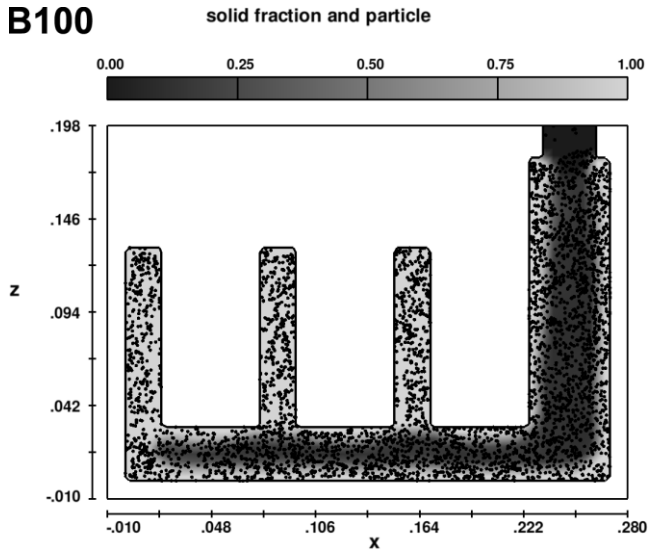

Fig. 6b. Two dimensional distribution of particles type B100 (black points) after 150 [s]

3.2. Particles type B

In the second case where particle density was equal to the density of liquid alloy, distributions of particles type B100 and B10 after filling and solidification were similar and homogenous in the system (Fig. 6a-b).

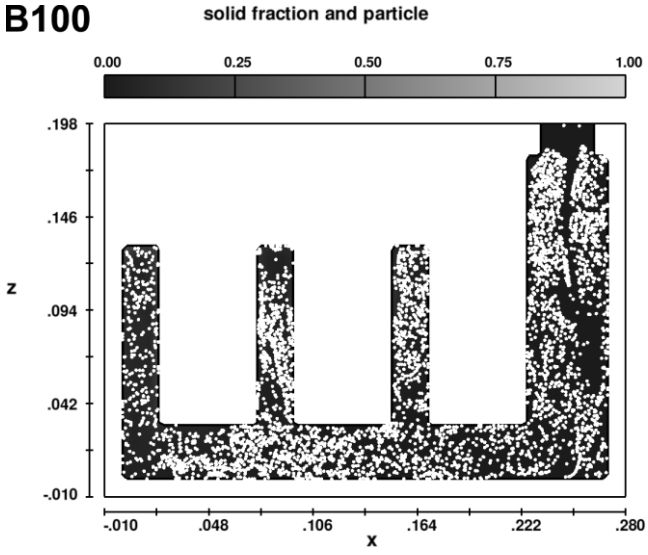

Fig. 6a. Two dimensional distribution of particles type B100 (white points) after 5.5 [s]

3.3. Particles type C

The figures 7a and 7b shows a visualization of computed particle distribution in the case, when particles density is two times greater than density of the liquid aluminum (particles type C100).

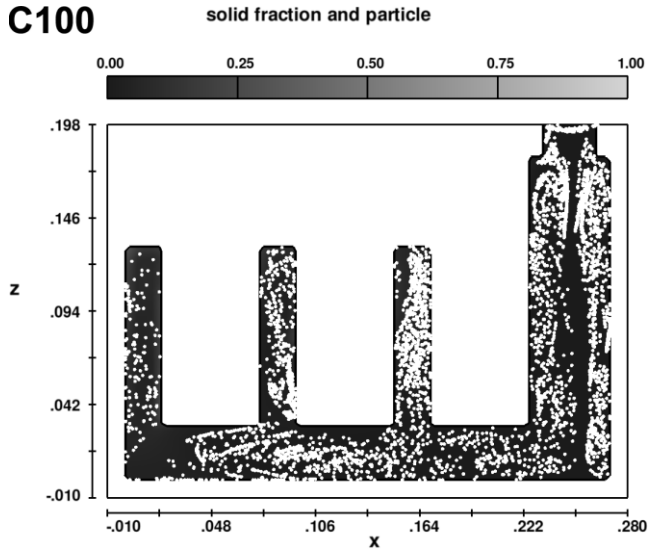

Fig. 7a. Two dimensional distribution of particles type C100 (white points) after 5.5 [s]

In this case immediately after filling (Fig.7a) particles starting to escapes from the upper part of the plates.

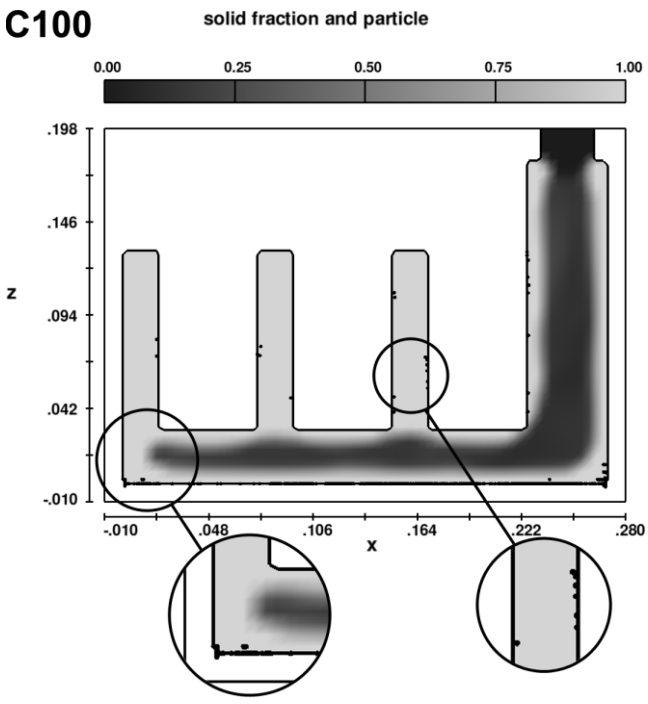

Fig. 7b. Two dimensional distribution of particles type C100 (black points) after 150 [s]; Visible magnification of selected areas of the plates and gating system

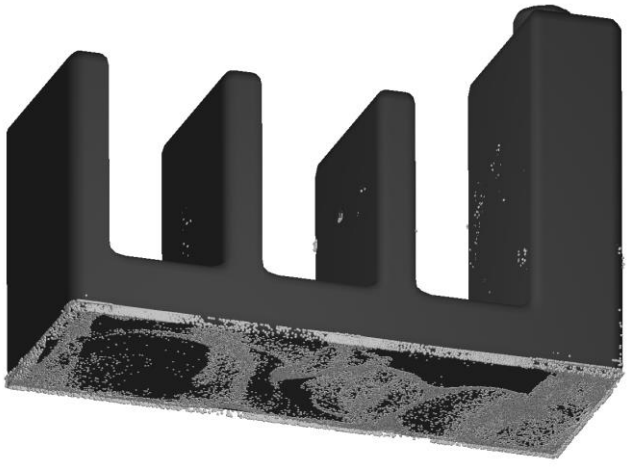

Fig. 8. Three dimensional distribution of particle C100 (white point) on the bottom of model system after 150 [s]

This process continues during the cooling and solidification. Hence, most of the C100 particles flows to the bottom of the model system. Only few single particles were "frozen" in solidified casts right after filling. Those particles can be observed in the plates No. 1-3 near the mould walls (Fig. 7b). This results in highest particles concentration in gating system (Fig. 8).

The last analyzed problem includes the particles with highest density and size of 10 [μm] (type C10). In this case during whole process particles distribution (Fig. 9a-b) was again close to uniform as in the A10 issue. Based on these two examples it can be assumed that to obtain homogenous distribution, large density difference between liquid alloy and particles must be compensated by smaller particles size.

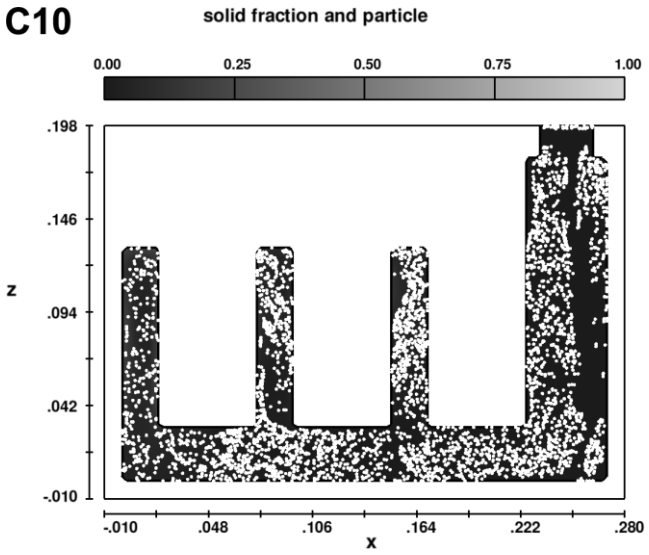

Fig. 9a. Two dimensional distribution of particles type C10 (white points) after 5.5 [s];

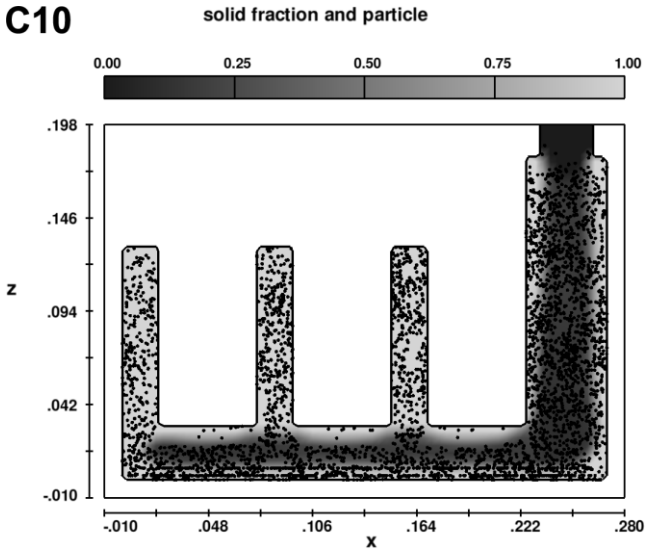

Fig. 9b. Two dimensional distribution of particles type C10 (black points) after 150 [s]

4. Conclusions

Final distribution of particles in the cast will be affected by both the filling process and particle movement during cooling and solidification. The most important factor influencing the behavior of the solid particles in the mould is their density and size in relation to the density of the liquid alloy. Additionally, in the case of significant density differences between analyzed phases, final particles location will depend on the cooling rate and temperature distribution in the system after filling. These parameters translate into a time in which the particles can change their location in a liquid metal. At the same time in such a case homogenous distribution can be still obtained by using particles with smaller diameter.

Acknowledgements

The authors acknowledge financial support from Polish National Science Centre through grant No. 2011/03/B/ST8/05020.

References

[1] Hashim, J., Looney, L., Hashmi, M.S.J. (2002). Particle distribution in cast metal matrix composites-Part I. *Journal of Materials Processing Technology*, 123, 251-257 DOI: 10.1016/S0924-0136(02)00098-5

[2] Lelito, J., Żak, P.L., Greer, A.L., Suchy, J.S. Krajewski, W.K., Gracz, B., Szucki, M., Shirzadi, A.A. (2012). Crystallization model of magnesium primary phase in the AZ91/SiC composite. *Composites Part B: Engineering*, 43, 3306-3309. DOI: 10.1016/j.compositesb.2012.01.088

[3] Lelito, J., Żak, P.L., Shirzadi, A.A., Greer, A.L., Krajewski, W.K., Suchy, J.S., Haberl, K., Schumacher, P. (2012) Effect of SiC reinforcement particles on the grain density in a magnesium-based metal–matrix composite: Modelling and experiment. *Acta Materialia*, 60, 2950-2958. DOI: 10.1016/j.actamat.2012.01. 058

[4] Pasieka, A., Konopka, Z. (2013) The Influence of Pressure Die Casting Parameters on Distribution of Reinforcing Particles in the AlSi11/10% SiC Composite. Archives of Foundry Engineering, 13(3), 64-67. DOI: 10.2478/afe-2013-0061

[5] Xu, Z., Yan, J., Liu, J., Yang, S. (2008). Floating of SiC particles in a Zn–Al filler metal. *Materials Science and Engineering A*, 474, 157-164. DOI: 10.1016/j.msea.2007.05. 088

[6] Cetin, A., Kalkanli, A. (2009). Numerical simulation of solidification kinetics in A356/SiCp composites for assessment of as-cast particle distribution. J*ournal of Materials Processing Technology*, 209, 4795-4801. DOI: 10.1016/j.jmatprotec.2008.12.007

[7] Reilly, C., Jolly, M.R., Green, N.R., Gebelin, J.C., (2010). Assessment of Casting Filling by Modeling Surface Entrainment Events Using CFD. In TMS Annual Meeting & Exhibition, 14-18 February, 2010. Seattle, Washington, USA

[8] Nath, D., Asthana, R., Rohatgi, P.K. (1987). Particle distribution control in cast aluminium alloy-mica composites. *Journal of Material Science*, 22(1), 170-176. DOI: 10.1007/BF01160567